



**University of
Zurich**^{UZH}

**Zurich Open Repository and
Archive**

University of Zurich
University Library
Strickhofstrasse 39
CH-8057 Zurich
www.zora.uzh.ch

Year: 2023

Transplantation of porcine adrenal spheroids for the treatment of adrenal insufficiency

Malyukov, Maria ; Gelfgat, Evgeny ; Ruiz-Babot, Gerard ; Schmid, Janine ; Lehmann, Susann ; Spinas, Giatgen ;
Beuschlein, Felix ; Hantel, Constanze ; Reisch, Nicole ; Nawroth, Peter Paul ; Bornstein, Stefan R ; Steenblock,
Charlotte ; Ludwig, Barbara

DOI: <https://doi.org/10.1111/xen.12819>

Posted at the Zurich Open Repository and Archive, University of Zurich

ZORA URL: <https://doi.org/10.5167/uzh-255572>

Journal Article

Published Version



The following work is licensed under a Creative Commons: Attribution-NonCommercial-NoDerivatives 4.0 International (CC BY-NC-ND 4.0) License.

Originally published at:

Malyukov, Maria; Gelfgat, Evgeny; Ruiz-Babot, Gerard; Schmid, Janine; Lehmann, Susann; Spinas, Giatgen; Beuschlein, Felix; Hantel, Constanze; Reisch, Nicole; Nawroth, Peter Paul; Bornstein, Stefan R; Steenblock, Charlotte; Ludwig, Barbara (2023). Transplantation of porcine adrenal spheroids for the treatment of adrenal insufficiency. *Xenotransplantation*, 30(5):e12819.

DOI: <https://doi.org/10.1111/xen.12819>

Transplantation of porcine adrenal spheroids for the treatment of adrenal insufficiency

Maria Malyukov¹  | Evgeny Gelfgat¹ | Gerard Ruiz-Babot¹ | Janine Schmid¹ |
 Susann Lehmann¹ | Giatgen Spinas² | Felix Beuschlein³ | Constanze Hantel^{1,3} |
 Nicole Reisch⁴ | Peter P. Nawroth⁵ | Stefan R. Bornstein^{1,6} |
 Charlotte Steenblock¹  | Barbara Ludwig^{1,3,7,8}

¹Department of Internal Medicine III, University Hospital Carl Gustav Carus, Technical University Dresden, Dresden, Germany

²Medical Faculty, University Hospital Zürich, Zürich, Switzerland

³Department of Endocrinology, Diabetology and Clinical Nutrition, University Hospital Zürich, Zürich, Switzerland

⁴Medizinische Klinik IV, Klinikum der Universität München, Munich, Germany

⁵Medical Faculty Heidelberg, University Hospital Heidelberg, Heidelberg, Germany

⁶Faculty of Life Sciences & Medicine, School of Cardiovascular and Metabolic Medicine and Sciences, King's College London, London, UK

⁷Paul Langerhans Institute Dresden of Helmholtz Centre Munich at University Hospital Carl Gustav Carus of TU Dresden Faculty of Medicine, Dresden, Germany

⁸DFG-Center for Regenerative Therapies Dresden, Technical University Dresden, Dresden, Germany

Correspondence

Maria Malyukov, Department of Internal Medicine III, University Hospital Carl Gustav Carus, Technical University Dresden, Fetscherstrasse 74, 01307 Dresden, Germany.
 Email:
Maria.Malyukov@uniklinikum-dresden.de

Funding information

Deutsche Forschungsgemeinschaft (DFG, German Research Foundation), Grant/Award Number: 314061271 TRR 205; TransCampus initiative between TU Dresden and King's College London; TransCampus initiative between TU Dresden and King's College London; Deutsche Forschungsgemeinschaft; Deutscher Akademischer Austauschdienst

Abstract

Primary adrenal insufficiency is a life-threatening disorder, which requires lifelong hormone replacement therapy. Transplantation of xenogeneic adrenal cells is a potential alternative approach for the treatment of adrenal insufficiency. For a successful outcome of this replacement therapy, transplanted cells should provide adequate hormone secretion and respond to adrenal physiological stimuli. Here, we describe the generation and characterization of primary porcine adrenal spheroids capable of replacing the function of adrenal glands in vivo. Cells within the spheroids morphologically resembled adult adrenocortical cells and synthesized and secreted adrenal steroid hormones in a regulated manner. Moreover, the embedding of the spheroids in alginate led to the formation of cellular elongations of steroidogenic cells migrating centripetally towards the inner part of the slab, similar to zona Fasciculata cells in the intact organ. Finally, transplantation of adrenal spheroids in adrenalectomized SCID mice reversed the adrenal insufficiency phenotype, which significantly improved animals' survival. Overall, such adrenal models could be employed for disease modeling and drug testing, and represent the first step toward potential clinical trials in the future.

Abbreviations: ACTH, adrenocorticotrophic hormone; Ang II, angiotensin II; zF, zona Fasciculata; zG, zona Glomerulosa; zR, zona Reticularis.

Maria Malyukov and Evgeny Gelfgat authors contributed equally to this work.

This is an open access article under the terms of the [Creative Commons Attribution-NonCommercial-NoDerivs](https://creativecommons.org/licenses/by-nc-nd/4.0/) License, which permits use and distribution in any medium, provided the original work is properly cited, the use is non-commercial and no modifications or adaptations are made.

© 2023 The Authors. *Xenotransplantation* published by John Wiley & Sons Ltd.

KEYWORDS

adrenal gland, adrenal insufficiency, adrenocortical stem and progenitor cells, multicellular spheroids, xenogeneic transplantation

1 | INTRODUCTION

Adrenal insufficiency is a rare condition, with an estimated prevalence of 82–144 cases per million people in the general population.¹ The adrenal glands of patients suffering from adrenal insufficiency are unable to produce adequate amounts of steroid hormones. Currently, the only treatment option for affected patients is hormone substitution. Pharmacological treatment with glucocorticoids might lead to undesirable side effects, such as hypertension, overweight, reduced glucose tolerance, diabetes mellitus, and ultimately increased mortality in cardiovascular disease.² At the same time, mineralocorticoid deficiency in patients with primary adrenal insufficiency can result in hypotension, weakness, salt craving, and electrolyte disturbances, such as hypokalemia and hyponatremia.³ Dose adjustments are frequently needed, especially in intercurrent illness, surgery, pregnancy, and other situations of stress.³ Moreover, patients with adrenal insufficiency are at risk of adrenal crises. Adrenal crisis, also known as Addisonian crisis, is a life-threatening condition with an estimated incidence of 6 to 8 cases per 100 patient-years.⁴ It involves rapid progression from non-specific symptoms, such as fatigue, weakness, nausea, vomiting, abdominal pain, back pain, diarrhea, dizziness, and hypotension, to a hypotensive crisis and possibly metabolic encephalopathy and shock. Therefore, a novel treatment strategy for adrenal insufficiency is urgently needed.

One promising approach might be the transplantation of adrenal spheroids or organoids, whereby the amount and timing of the release of steroid hormones are precisely regulated by the hypothalamic-pituitary-adrenal axis (HPA) and renin-angiotensin-aldosterone axis (RAAS) of the host. In the past decade, the concept of spheroid transplantation was successfully applied for the treatment of numerous pathological conditions, such as acute liver failure, synovitis, fat pad fibrosis, or type 1 diabetes.^{5–7} In the adrenal field, several studies have used cell replacement strategies to treat adrenal insufficiency.^{8–11} However, in the majority of cases, transplantations were unable to fully restore adrenal hormone production under normal physiological regulation, which can be attributed to the diminished production of mineralocorticoids.

For successful transplantation experiments, the cell source of choice is of crucial importance. Rodent-derived cell sources cannot model potential human cell replacement therapies due to species-related differences; unlike humans, the mouse adrenal lacks zona reticularis (zR) and as a result, DHEA and androgen production¹² (Figure S1A). Moreover, due to the absence of the enzyme 17 α -hydroxylase, rodent adrenal cells produce corticosterone instead of cortisol¹² (Figure S1A). When using cortisol-producing cells and rodents as a host for adrenal replacement strategies that becomes a big advantage, since

cortisol in rodent plasma could be only produced by transplanted cells.

Previous experiments using primary bovine adrenocortical cells encapsulated in alginate,^{10,13} successfully reversed induced adrenal insufficiency in rodents.¹⁰ However, these experiments would not go beyond preclinical trials since bovine cell sources do not meet the safety requirements for potential clinical applications. Thus, new sources of adrenocortical cells mimicking human adrenal structure and physiology are highly needed. Porcine adrenals have three adrenal zones and the majority of steroidogenic enzymes, which are present in humans^{14,15} (Figure S1B,C). Within the last decade, steady progress has been made in the development of donor pigs optimal for transplantation. These models involved the establishment of “designated pathogen-free” herds and inactivation of porcine endogenous retroviruses using the CRISPR/Cas9 technology and blastocyst complementation,^{16,17} thus paving the way for clinical trials of porcine organ or cell transplantation into humans.

Here, we report the development and characterization of a porcine multicellular adrenal spheroid model. Additionally, we investigated the model's regenerative and therapeutic potential in vivo.

2 | MATERIALS AND METHODS

2.1 | Cell isolation and cultivation

Porcine adrenal cells were isolated from the adrenal glands of freshly sacrificed pigs at approximately 6 months of age. The glands were transported to the laboratory in cold Euro-Collins solution containing 1% (vol/vol) of penicillin-streptomycin-nystatin (the solution contained 10 000 U/mL Pen., 10 mg/mL Strep., 1250 U/mL Nystatin) (Neolab), freed of connective and adipose tissue and washed twice with phosphate-buffered saline (PBS, Gibco, Thermo Fisher Scientific). Following, the glands were cut in halves by a longitudinal incision, and the cortex with medulla was scraped off the capsule, cut into small pieces, and digested for 50 min in Dulbecco's Modified Eagle Medium: Nutrient Mixture F12 (DMEM/F12, Gibco, Thermo Fisher Scientific), containing 2 mg/mL collagenase type V (Merck), and 0.1 mg/mL DNase (Roche) at 37°C while shaking. In the next step, the cells were washed twice in standard cultivation medium (DMEM/F12 with 5% (vol/vol) heat-inactivated fetal bovine serum (FBS), 10% (vol/vol) horse serum (both from Gibco, Thermo Fisher Scientific), 10 μ g/mL insulin (Sanofi), 5 μ g/mL transferrin (Merck), and 1% (vol/vol) penicillin-streptomycin-nystatin, pelleted by centrifugation (8 min, 300 \times g) and filtered through gauze. Primary adrenal cells were cultivated in

standard cultivation medium in culture flasks at 37°C in a humidified atmosphere (95% air, 5% CO₂). On the next day, cells were trypsinized (TrypLE™, Thermo Fisher Scientific), pelleted by centrifugation, resuspended in a freezing medium (standard cultivation medium, containing 10% (vol/vol) dimethyl sulfoxide), and stored in liquid nitrogen.

2.2 | Spheroid formation

Frozen cells were thawed, resuspended in standard cultivation medium, and cultivated in culture flasks for 4 days. Following, the cells were trypsinized and seeded in AggreWell plates (Stemcell Technologies), prepared according to the manufacturer's instructions, for overnight cultivation (200 cells per microwell) in 500 µL of standard cultivation medium per well.

2.3 | Spheroid or suspension cell encapsulation and cultivation

Cell encapsulation in alginate has been previously described.¹⁰ The day after spheroid formation, spheroids were mixed gently with 150 µL of 2% Pronova sodium alginate (Novamatrix). Then 30 µL of the mixture was placed on a glass plate with 550 µm spacers, covered with flat Sintered glass (Pyrex), and cross-linked with 70 mM strontium chloride, containing 20 mM HEPES, for 10 min. Alginate slabs were cultivated in neurobasal medium (Neurobasal medium, containing 2% (vol/vol) of B-27 supplement, 2 mM L-glutamine (all from Thermo Fisher Scientific), 20 ng/mL fibroblast growth factor 2 (FGF-2, Promocell) and 1% (vol/vol) penicillin-streptomycin-nystatin). Each alginate slab contained spheroids formed from 200,000 cells. Spheroids with extensions were generated by cultivation of the alginate slabs with adrenal spheroids in the neurobasal medium for 3 weeks.

2.4 | Adrenalectomy and transplantation

Female SCID mice (8 weeks old) were obtained from Charles River Laboratory. The group of mice assigned to the control condition ($n = 4$) did not receive any treatment, thus remaining unaffected by any intervention. The experimental mice ($n = 28$) were anesthetized by ketamine/xylazine. Adrenalectomy and transplantation were performed in one surgery. A longitudinal incision was made in the dorsal skin of the retrocostal area. An incision approximately 1 cm long was made in each lateral body to open the retroperitoneal space. Following, the adrenal glands were located and removed.

Experimental animals were divided into four groups and received transplantation of 1×10^6 cells (Table 1): (1) cell suspension of porcine adrenal cells ($n = 6$), (2) naked adrenal spheroids ($n = 10$), (3) alginate slabs with freshly encapsulated spheroids ($n = 6$), or (4) spheroids

TABLE 1 Groups of animals with transplanted porcine adrenal cells and spheroids.

Group	Transplant	Group size
1	Cell suspension	$n = 6$
2	Naked spheroids	$n = 10$
3	Freshly alginate-encapsulated spheroids	$n = 6$
4	Spheroids encapsulated and cultivated for 3 weeks	$n = 6$
5	Control (no intervention)	$n = 4$

encapsulated in alginate and cultivated for 3 weeks to allow for extension growth ($n = 6$).

The estimation of cell numbers was conducted as follows: for group 1, the count of individual cells was performed at the time of transplantation. In the case of groups 2 and 3, cell counting was carried out during spheroid formation, 24 h prior to transplantation, and the corresponding number of spheroids was subsequently utilized. For group 4, cell counting was conducted during spheroid formation, 24 h before the spheroids were embedded in alginate and cultivated for a duration of 3 weeks. Throughout this period, cellular proliferation took place.

For transplantation, a small scratch was performed in the kidney capsule, and the capsule was gently separated from the kidney. In the case of experimental groups 1 and 2, cells or spheroids were infused in 20 µL of fibrinogen (10 mg/mL)/thrombin (10 U/mL) (both from Merck) mixture in the formed porch of the left kidney. In the case of experimental groups 3 and 4, slabs were directly inserted in the formed porch, with each mouse receiving two identical slabs, each containing spheroids with or without extensions, respectively, formed from 5×10^5 cells, one underneath each kidney capsule (two slabs per animal). Following, the retroperitoneal space and the skin were closed with stitches.

2.5 | Post-transplantation follow-up

Following the surgical procedure, the animals were maintained on a standard diet without additional salt supplementation. Animals were monitored for up to 31 days after transplantation. During the first 7 postoperative days, all experimental mice received intraperitoneal (i.p.) injections of dexamethasone in decreasing doses. Within the initial 3 days following the surgical procedure, the mice received injections at a dosage of 1 µg/g of body weight. For the subsequent 2 days, the dosage was adjusted to 0.75 µg/g. Finally, for the following 2 days, the dosage was further reduced to 0.5 µg/g of body weight.

ACTH-tests were performed on days 11, 21, and before the end of the trial (day 31 after the transplantation). ACTH (Synacthen, Sigma-tau Arzneimittel GmbH) was dissolved in 0.9% NaCl to the final concentration of 2 µg/mL and was injected i.p. at a dose of 2 µg/kg body weight. Blood samples were taken from the tail tip 30 min after Synacthen injection.

At the termination of the experiment, a thorough analysis was conducted on all samples that were embedded in alginate. However, it was found to be difficult to locate and retrieve the transplants from mice in groups 1 and 2, rendering them ineligible for analysis.

2.6 | Steroid and catecholamine release and measurement

2.6.1 | In vitro experiments

For basal and ACTH-stimulated steroid release, the monolayer culture of cells (100,000 cells per well) or slabs (originally ~1000 spheroids of 200 cells each per slab) were incubated in 0.5 mL (monolayer culture) or 1 mL (slabs) of cultivation medium with or without the addition of 3 ng/mL ACTH₁₋₂₄ (Synacthen, Sigma-tau Arzneimittel GmbH) for 24 h. Angiotensin II (Merck) was used in a concentration of 10⁻⁷ M for 24 h. The concentrations of cortisol or aldosterone in the cell culture supernatants were determined by cortisol (IBL, RE52061) or aldosterone ELISA (IBL, RE52301). To perform the steroid hormone assay, the samples were cultivated in a fresh neurobasal medium, which is a serum-free medium. It is important to note that the level of cortisol in this particular medium was found to be below the detection limit. Cell sensitivity to ACTH (stimulation index) was calculated by dividing the stimulated values of corticosteroids by basal ones.

Dopamine was measured in the cell culture supernatant of adrenal cells, seeded in the density of 100,000 cells per well, and cultivated as a monolayer in standard cultivation medium by Dopamine ELISA (IBL, RE59161). Fresh medium was added to the cells 24 h before the collection time.

2.6.2 | In vivo experiments

Due to the low amount of blood collected on days 11 and 21 of the trial, the steroid profile of the samples could not be measured by liquid chromatography with tandem mass spectrometry (LC-MS/MS) analysis, and the level of cortisol was measured by cortisol ELISA (IBL, RE52611). At the endpoint of the experiment, the steroid profile was detected by LC-MS/MS as previously described.¹⁸

2.7 | Reverse-transcription and semi-quantitative real-time PCR

Total RNA from adrenocortical cells was isolated using the RNeasy Mini Kit (Qiagen) following the manufacturer's instructions. RNA was converted to first-strand cDNA by a reverse transcription system (Promega). Primers were designed using Primer-BLAST—NCBI software to span at least one intron to prevent nonspecific amplification

of DNA remnants. Semi-quantitative real-time PCR was performed utilizing SYBR green (Qiagen) and a Roche Light Cycler 1.5 (Roche). Each sample was analyzed in four replicates. To normalize data, the *RPS9* gene was used as an internal control gene. The primers used are presented in Table 2.

2.8 | Viability staining

Fluorescein diacetate (FDA) and propidium iodide (PI) staining was used to define the viability of porcine spheroids. Stained spheroids were examined under the microscope (Axioplan, Carl Zeiss). Analysis was performed using Axiovision Software (Carl Zeiss). Viability was defined by the quantification of live (FDA-green) and dead (PI-red) cells.

2.9 | Immunofluorescence staining and microscopy

Cultivated cells were fixed with 4% paraformaldehyde (PFA) for 20 min in the room temperature. After application of permeabilization and blocking solution, the cells were incubated with appropriate primary antibody overnight at 4°C. After blocking with PBS, containing 0.02% saponin, the samples were incubated with the appropriate fluorophore-conjugated secondary antibodies (Rabbit Cy3 or Mouse A647) in PBS for 2 h at room temperature. DAPI (Roche) was used for cell nucleus-specific staining. Then the samples were mounted with Aqua-Poly/Mount (Polysciences).

Freshly prepared free-floating adrenal spheroids were embedded in 4% agarose in PBS, fixed overnight in 4% PFA (ChemCruz), and embedded in paraffin. Samples encapsulated in alginate were washed with PBS and fixed for 1 h in 4% PFA and then alginate was dissolved by 0.1 M EDTA. Following, released spheroids with extensions were embedded in paraffin. Porcine adrenals were fixed overnight in 10% formalin solution (Merck) and embedded in paraffin. Paraffin slides were rehydrated with descending concentrations of ethanol and incubated for 5 min in PBS before antigen retrieval (10 min boiling in Tris-EDTA buffer, pH 9.0). Blocking was performed with 0.3% Tween-20 (Merck), 0.5% bovine serum albumin (BSA, Merck), 10% normal goat serum (Merck) in PBS, for 1 h at room temperature. Immunohistochemistry was performed on 6- μ m sections using respective primary antibodies at 4°C overnight (Table 3). After washing in PBS with 0.5% Tween 20, the samples were incubated with the appropriate fluorophore-conjugated secondary antibodies in PBS for 2 h at room temperature. DAPI (Roche) was used for cell nucleus-specific staining. The negative control underwent an identical processing protocol, but omitting the primary antibody. Immunofluorescence microscopy was performed on a Zeiss Axiovert 200 M microscope with an AxioCamMRc5 camera using ZEN 3.3 (Carl Zeiss) software. The primary antibodies employed in this study underwent validation procedures using native porcine adrenals (Figure S2).

TABLE 2 List of primers and amplification conditions for RT-PCR.

Gene	Primer sequence	Annealing Temperature, °C	Product size (bp)
RPS9	F: GACGTCAGCAGACGGCAA R: GAGCCCATATTCCGCCGATCA	65	216
DAX1	F: CGTGCTCTTTAATCCGGACCT R: CAGCTCCTGTAAGTGGGTGG	65	293
GLI1	F: CAGGCAACCGTGATCTCTT R: TGAGGGAACGCTCTGGAGTA	65	145
CTNNB1	F: GAGACGGAGGAAGTCCGAG R: GAGATCCTCAGGGGAACAGG	60	110
WNT4	F: AGTCCACTTCCAGGACCCACG R: CGGGTCCCTTGTCACCACCTT	60	356
CYP21	F: AGCCCAACCTCCCATCTAT R: AGACGCCAGCTGTAGGATG	60	182
CYP17A1	F: CAGCCTCTCTCTGGCGAT R: AGTTTCTGCTGTAGTTCTCCTTACG	65	268

TABLE 3 Antibodies used in this study.

Antibody	Manufacturer	Catalog Nr.	Host and clonality	Species reactivity	Dilution
Ki67	Abcam	ab15580	Rabbit polyclonal	M, Hu, R, S, Rab, Ho, Bo, D, P, Mon, Ha	1:100
SF-1	Cosmo Bio USA	KAL-KO611	Rabbit polyclonal	C, M	1:100
StAR	Cell Signaling	cs-8449	Rabbit monoclonal	M, R, Hu	1:100
CYP11B1	Merck	HPA056348	Rabbit polyclonal	Hu	1:100
TOM20	Santa Cruz Biotechnology	sc-11415	Rabbit polyclonal	M, R, Hu, Ho, D, P, A	1:100
TH	Abcam	ab112	Rabbit polyclonal	R, Ma	1:200
Vimentin	Abcam	ab8978	Mouse monoclonal	M, R, G, Chi, Ha, C, Hu, F, Mon, Z	1:100
Fibronectin	Abcam	ab27224	Chicken polyclonal	M, R, Hu	1:100
CYP11A1	Cell Signaling	cs-14217	Rabbit monoclonal	Hu, M, R	1:100
Donkey anti-Rabbit IgG	Invitrogen	A31573	Donkey		1:400
Donkey Anti-Mouse IgG	Jackson Immunoresearch	715-585-151	Donkey		1:400
Goat anti-Chicken IgY	Invitrogen	A32933	Goat		1:400

Abbreviations: A, Avian; Chi, Chicken; C, Cow; D, Dog; F, Frog; G, Goat; Ha, Hamster; Ho, Horse; Hu, Human; Ma, Mammals; M, Mouse; Mon, Monkey; P, Pig; R, Rat; Rab, Rabbit; S, Sheep; Z, Zebrafish.

2.10 | Transmission electron microscopy

Adrenal spheroids with extensions were fixed in 4% PFA in 0.1 M phosphate buffer (PB, pH 7.4), followed by post-fixation in modified Karnovsky's fixative (2% glutaraldehyde + 2% PFA in 50 mM HEPES, pH 7.4) overnight at 4°C.^{19,20} Samples were washed 2× in 100 mM phosphate buffer and 2× in water and post-fixed in 2% aqueous OsO₄ solution containing 1.5% potassium ferrocyanide and 2 mM CaCl₂ for 30 min on ice. After several washes with water, the samples were incubated in 1% thiocarbonylhydrazide in water (20 min at room

temperature), followed by washes in water and a second osmium contrasting step in 2% OsO₄/water (30 min, on ice). Samples were washed in water, en-bloc contrasted with 1% uranyl acetate/water for 2 h on ice, washed again in water, dehydrated in a graded series of ethanol/water (30%, 50%, 70%, 90%, 96%, 3 × 100% ethanol (pure ethanol on molecular sieve), and infiltrated in the epon substitute EMBed 812 (epon/ethanol mixtures: 1:3, 1:1, 3:1 for 1.5 h each, pure resin overnight, pure resin 5 h). Finally, the samples were embedded in flat embedding molds and cured at 65°C overnight. Ultrathin sections were prepared with a Leica UC6 ultramicrotome (Leica Microsystems,

Vienna, Austria), collected on formvar-coated slot grids, and stained with lead citrate²¹ and uranyl acetate. Contrast-enhanced ultrathin sections were analyzed on a Jeol JEM1400 Plus (JEOL, Freising, Germany, camera: Ruby, JEOL) running with 80 kV acceleration voltage.

2.11 | Statistical analyses

Quantitative data is represented as mean \pm SEM. Statistical significance was determined by a two-tailed Student's *t*-test, Mann-Whitney *U* test, Wilcoxon signed-rank test, Fisher's exact test, or one-way Analysis of Variance (ANOVA) with a post hoc Bonferroni's multiple comparison test where appropriate by using GraphPad Prism 8 or SPSS software. To determine the appropriate number of animals required for our *in vivo* experiment, power calculations utilizing a two-tailed Student's *t*-test were conducted using the program G*Power 3.1. A value of $p \leq .05$ was considered significant in all tests.

2.12 | Study approval

All animal experiments were performed in strict accordance with animal protocols (25-5131/354/28) approved 28.07.2016 by the ethical and research board of the Landesdirektion Sachsen. The ethical and research board of the Landesdirektion Sachsen did not approve the use of negative control (sham transplanted adrenalectomized animals). Adrenalectomy is known to have severe consequences, as documented in the literature. Conducting additional experiments involving adrenalectomy would cause unnecessary harm and suffering to the animals involved.

3 | RESULTS

3.1 | Determination of the optimal time point for porcine adrenal spheroid formation

We have previously shown that progenitor cells are an important component of functionally active spheroids.¹³ Therefore, we analyzed the dynamics of the relative gene expression of several progenitor cell markers, such as *GLI1*, *DAX1*, *WNT4*, and β -catenin (*CTNNB1*). We detected significant upregulation of *DAX1* ($p < .01$, Figure 1A) on day 4, compared to day 1 after cell isolation. Then gene expression of *DAX1* was significantly downregulated on day 7 compared to day 4 ($p < .05$, Figure 1A). Gene expression of *CTNNB1*, *GLI1*, and *WNT4* had a tendency toward increase on days 4 and 7, which, however, did not reach significance (Figure 1B–D).

Next, we examined the expression of the steroidogenic enzymes *CYP21* and *CYP17A1*, relevant for cortisol, aldosterone, and adrenal androgen production, in primary adrenocortical cells cultured as a monolayer on days 1, 4, and 7 after isolation. The expression of *CYP21* and *CYP17A1* was significantly elevated on day 4 ($p < .01$, Figure 1E,F), and then downregulated on day 7, compared to day 4 ($p < .05$ for

CYP17A1 and $p > .05$ for *CYP21*). Adrenal steroid synthesis is under the control of adrenocorticotrophic hormone (ACTH). The cell sensitivity to ACTH (stimulation index) reached its maximum on day 4 for both cortisol (1.6) and aldosterone (1.7) (Figure 1G,H).

Until now, it was not possible to stably culture primary adrenocortical cells, which can synthesize cortisol, aldosterone, and adrenal androgens over an extended period of time. When monolayer cultures were kept for a longer time, the cellular properties were less optimal for spheroid formation, since the cells showed a reduced secretion of cortisol and aldosterone, likely due to the overgrowth of fibroblasts in the culture. Consistently, the responsiveness to ACTH on days 7, 10, and 14 was reduced (Figure 1G,H). To assess the presence of fibroblasts in our primary cultures, the steroidogenic marker SF-1 and the mesenchymal marker Vimentin were studied on days 4, 7, and 14. As shown in Figure S3, while on day 4, we mainly detected steroidogenic cell clusters, on day 14 the cultures were overgrown with fibroblasts. Thus, we selected day 4 as the optimal day for generating adrenal spheroids under the culture conditions used here.

In order to ascertain the presence of medullary cells, the supernatant from the adrenal cell culture monolayer was collected on days 4, 7, and 10. The collected samples were then assessed for dopamine levels, as depicted in Figure S4. It was observed that the dopamine concentration exhibited a tendency to decrease over the course of cultivation time.

3.2 | Multicellular adrenal spheroids contain stem cells and mature cortical and medullary cells

Spheroids were generated from primary cell cultures on day 4. Morphological analysis of formed spheroids showed a roundish shape approximately 80 μm ($79.6 \pm 0.7 \mu\text{m}$) in diameter (Figure 2A). FDA/PI staining demonstrated a cell viability higher than 90% (Figure 2B,C).

To meet the current therapeutic need, it is important that the adrenal spheroids contain cells expressing enzymes necessary for steroid production. Detailed characterization of the cell composition of the freshly prepared spheroids was performed by immunofluorescence staining, whereby a variety of different cell types was assessed. To determine the specificity of the antibodies, we first performed an immunofluorescence analysis on porcine adrenal sections with selected antibodies (Figure S2). Adrenal spheroids contained steroid-producing cells with a high number of TOM20-positive mitochondria, needed for steroidogenesis (Figure 2D). The steroidogenic cells were positively stained for SF-1, StAR, *CYP11A1*, and *CYP11B* (Figure 2E–H). SF-1, StAR, and *CYP11A1* take part in the steroid production of all steroid hormones: glucocorticoids, mineralocorticoids and androgens, and *CYP11B* is needed for cortisol and aldosterone production. In addition, we could detect TH-positive medullary cells (Figure 2I). Similarly, to bovine adrenocortical cells,²² porcine adrenal spheroids were able to synthesize fibronectin (Figure 2J). Moreover, spheroids contained Ki67-positive cells, which indicates cell proliferation (Figure 2K).

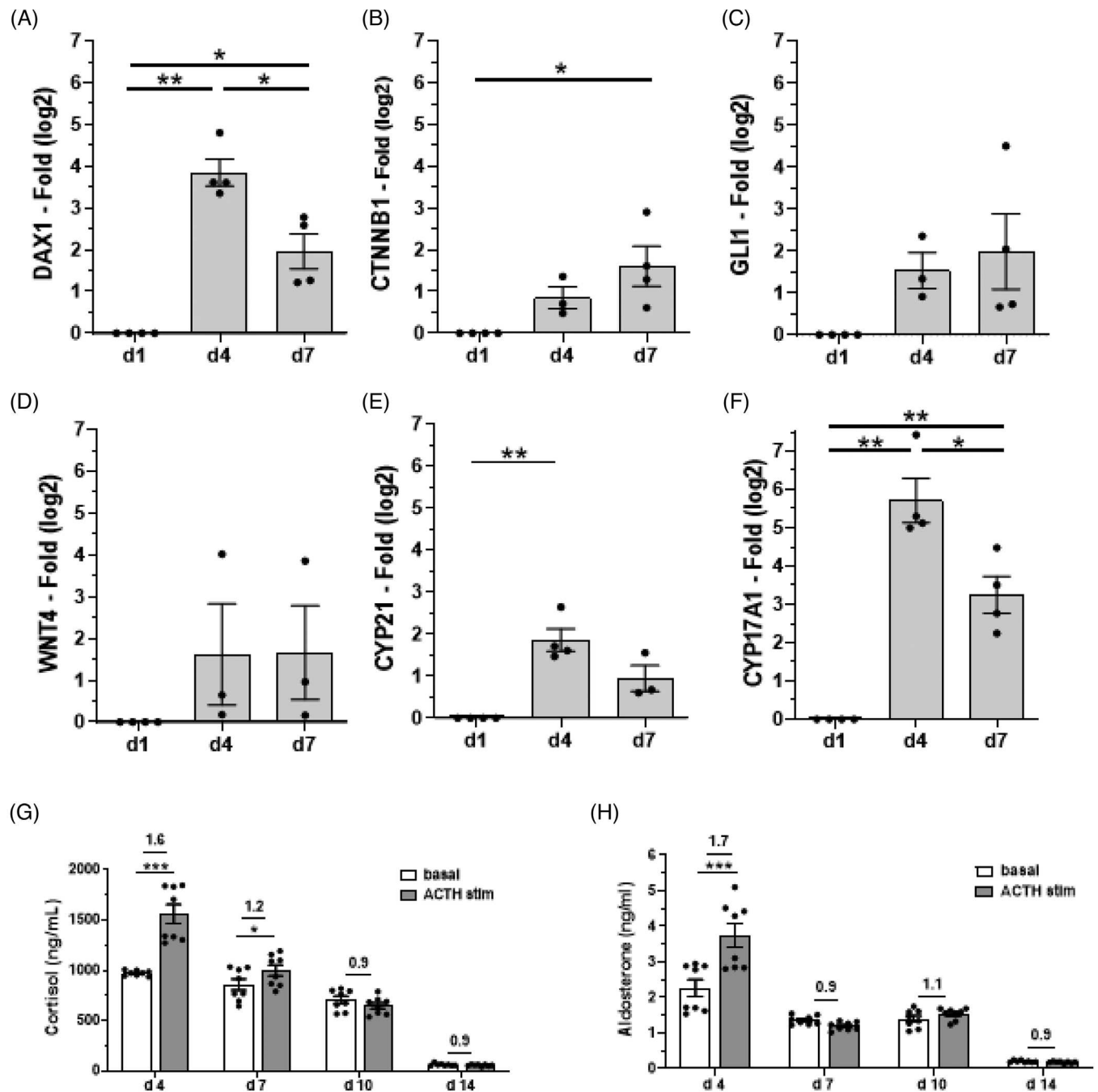


FIGURE 1 Determination of the optimal time point for spheroid formation. (A–D) Relative gene expression (log₂) of the progenitor markers (A) *DAX1*, (B) *CTNNB1*, (C) *GLI1*, and (D) *WNT4* of porcine adrenal cells cultivated for 1 day, 4 days, and 7 days in monolayer. (E, F) Relative gene expression analysis of specific steroidogenic hydroxylases, (E) *CYP21*, and (F) *CYP17A1* of adrenal cells cultivated for 1 day, 4 days, and 7 days ($n \geq 3$). (G, H) Basal and ACTH-induced secretion of cortisol and aldosterone of adrenal cells after cultivation in monolayer for 4 days, 7 days, 10 days, and 14 days ($n \geq 8$). Data are presented as mean \pm SEM. * $p < .05$, ** $p < .01$, *** $p < .001$.

3.3 | Adrenal spheroids form extensions after long-term cultivation

To achieve self-renewal of adrenal grafts, a continuous regeneration of hormone-synthesizing cells from stem cells is necessary. The presence of stem cells positively stained for *DAX1*, *SHH*, and *Nestin* in the spheroids was demonstrated previously.²³

Following the protocols established for bovine adrenocortical cells,^{10,24} porcine adrenal spheroids were encapsulated in alginate and cultivated for up to 10 weeks. Spheroids, located in the periphery of the alginate slabs, formed structures in the shape of columns, which grew centripetally (Figure 3A, B). The formation of the structures was induced by ACTH. ACTH (Synachten) was administered at the concentration of 3 ng/mL on a weekly basis for a duration of 24 h After

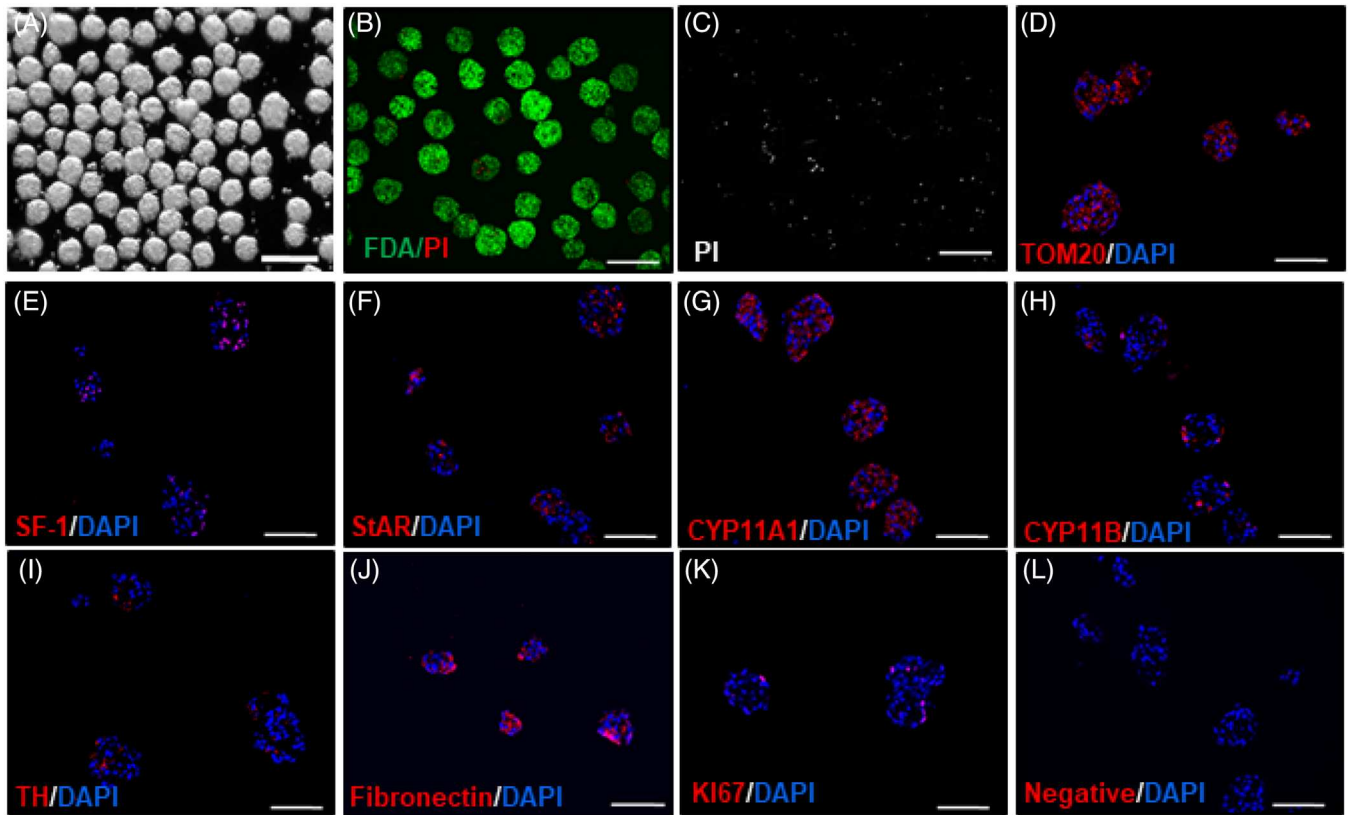


FIGURE 2 Structural characteristics of porcine adrenal spheroids. (A–C) scale bar 200 μm . (A) Light microscopy imaging. (B) Viability staining (FDA/PI). Live cells are stained green and dead cells - red. (C) Viability staining with PI. White represents dead cells. (D–L) Scale bar, 100 μm . (D) Staining for mitochondria with TOM20. (E–H) Staining for markers associated with steroid production (SF-1, StAR, CYP11A1, and CYP11B). (I) Staining for cell medullary cells (TH) (J) staining for fibronectin. (K) Ki67 staining for proliferation. (L) Negative control for D–K (minus primary antibody).

3 weeks, these structures reached a full length of up to 500 μm and stopped growing.

Morphologically, the structures were organized as chains of sequentially connected mature adrenocortical cells (Figure 3C), positive for SF-1 (Figure 3D–G). We observed cell proliferation within spheroids and the structures (Ki67-staining, Figure 3H–K). Further, electron-microscopical analysis of the cells inside these de novo formed extensions exhibited characteristic features of all three adrenal zones: zona Glomerulosa (zG) (Figure 4A), zona Fasciculata (zF) (Figure 4B) and zona Reticularis (zR) (Figure 4C), such as numerous cytoplasmic lipid droplets and mitochondria. The presence of elongated and oval-shaped cristae-like mitochondria is typical for the zG (Figure 4D), whereas round mitochondria with vesicular internal membranes are typical for zF cells (Figure 4E). Moreover, cells with an increased number of lysosomes and enlarged tubulovesicular mitochondria represent a hallmark of inner adrenocortical zR-like cells (Figure 4F).

Functional assessment of spheroids encapsulated in alginate was performed by investigating the effect of ACTH on the production of cortisol (Figure 4G) and aldosterone (Figure 4H). The average baseline synthesis for cortisol was 442 ± 36 ng/mL and 0.507 ± 0.02 ng/mL for aldosterone. When ACTH was added, average cortisol rose to

727 ± 41 ng/mL, and aldosterone to 0.856 ± 0.012 ng/mL. During the growth of adrenal extensions, which took place within the first 3 weeks of culture, both basal and ACTH-stimulated cortisol increased, whereas ACTH-stimulated aldosterone declined, following the stable steroid production till the end of the observation period. Alginate-encapsulated spheroids with extensions responded to specific stimulation with angiotensin II (Ang II) by significantly elevated aldosterone production (Figure 4I).

In the subsequent experimental analysis, we compared the steroid hormone secretion to the media collected at various time points between weeks 2 and 6 of cultivation. This assessment encompassed cell suspensions and spheroids both embedded in alginate. As illustrated in Figure 4J, the cellular suspensions and the spheroids exhibited similar levels of steroid hormone production, and no significant differences were observed between the two groups. Specifically, corticosterone and aldosterone, produced in cells derived from the zG, 11-deoxycortisol and cortisol produced in zF cells, and androstenedione and DHEA produced in zR cells, were synthesized. Notably, upon ACTH stimulation, there was a significant increase in glucocorticoid and mineralocorticoid production, while adrenal androgen production remained unaffected.

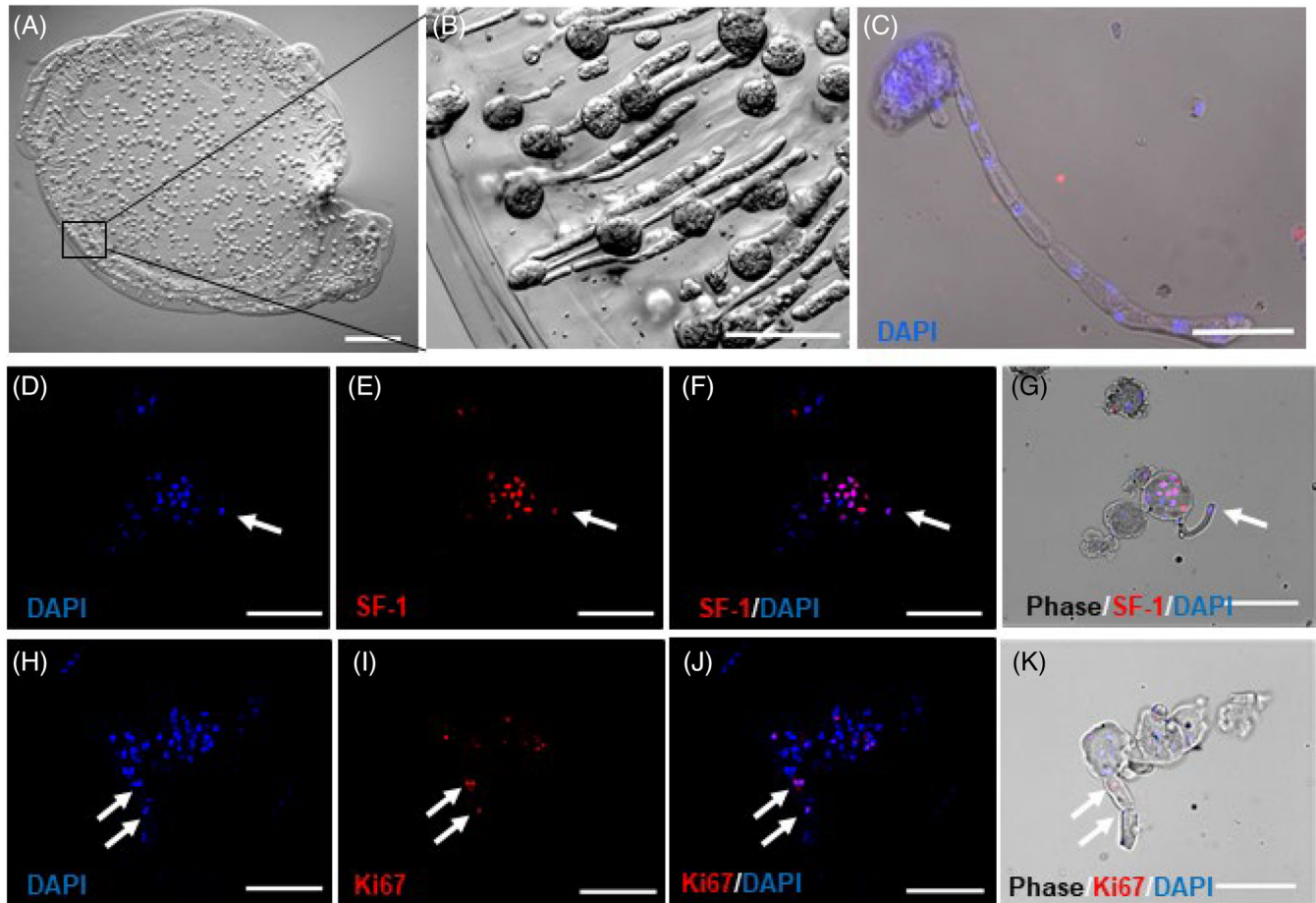


FIGURE 3 Encapsulated porcine spheroids form extensions. (A) Alginate slab with adrenal extensions, growing in the periphery towards the center of the slab (scale bar, 1000 μm). (B) Light microscopy of spheroids with extensions (scale bar, 100 μm). (C) Structure of extensions (DAPI staining plus light microscopy, scale bar, 100 μm). (D–G) Immunofluorescence staining of adrenal extensions for SF-1, associated with steroid production: (D)—location of the nuclei stained by DAPI, (E)—SF-1 staining, (F)—merged images of D and E, (G)—merged images of phase contrast and F (scale bar, 100 μm). (H–K) Immunofluorescence staining for Ki67, associated with proliferation: (H)—location of the nuclei stained by DAPI, (I)—Ki67 staining, (J)—merged images of H and I, (K)—merged images of phase contrast and J (scale bar, 100 μm). The arrows indicate areas of positive staining within the extensions.

3.4 | Transplanted porcine spheroids replace adrenal steroids in a mouse model of adrenal insufficiency

To assess the functional properties of the porcine spheroids *in vivo*, we used bilaterally adrenalectomized SCID mice ($n = 28$), which were categorized into four experimental groups (Table 1). Non-adrenalectomized mice ($n = 4$) were used as a negative control.

Previous studies on SCID mice demonstrated that 85%–90% of the animals die within 17 days after adrenalectomy.²⁵ In our experimental setting, two mice died (7%; one mouse from group 1 and one from group 4) during the post-transplantation follow-up (Figure S5A). One mouse (from group 1) exhibited an exceptionally low blood cortisol level (0.5 ng/mL), while the other deceased mouse (from group 3) displayed notably low body weight compared to the other animals in the group. Based on these observations, we suspect that both mice succumbed to adrenal insufficiency. The analysis of graft function in the deceased animals was not undertaken.

The steroid replacement potential of transplanted adrenal cells and spheroids was assessed by measuring plasma cortisol concentrations. In mice, corticosterone rather than cortisol is the predominant steroid. ELISA may still measure cortisol values in the blood of non-adrenalectomized mice at concentrations up to 0.15 ng/mL (when conducting 99% confidence interval) possibly due to cross-reactivity with other steroids. The excess of this statistical maximum was considered as a threshold value for the cortisol released by the transplants.

After transplantation, the plasma cortisol levels of all experimental SCID mice significantly exceeded the threshold value. Individual plasma cortisol levels were in the range of 0.25–5.26 ng/mL at all time points ($n = 78$). Porcine cell-derived cortisol was detected until the end of the experiment, that is, 31 days post-transplantation (Figure 5A and Figure S5B). Overall, throughout the observation period, animals that received transplantation of “naked” grafts (groups 1 and 2) exhibited a progressive increase in blood cortisol levels, whereas mice transplanted with freshly alginate-encapsulated spheroids (group 3) did

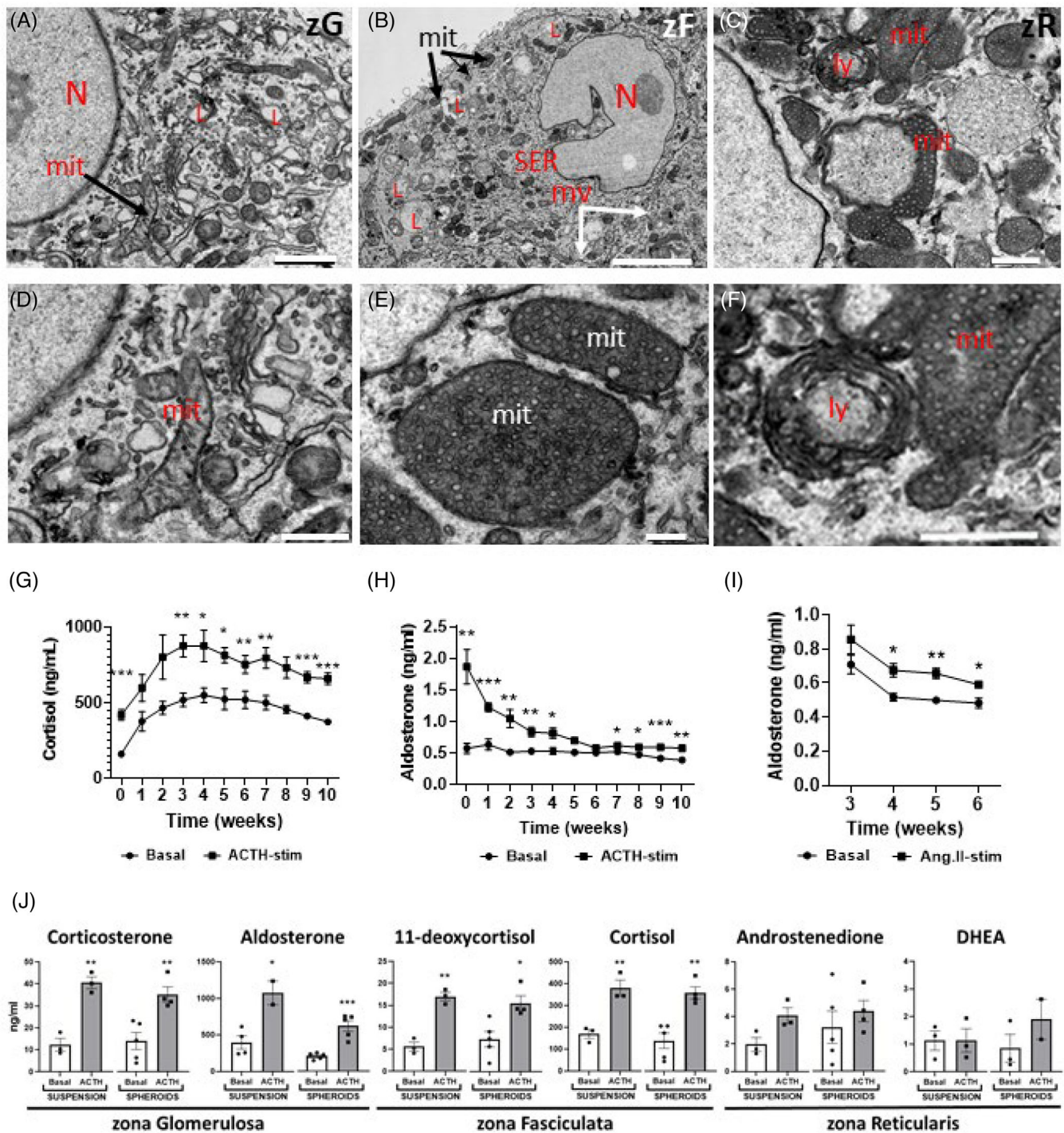


FIGURE 4 Electron micrographs of adrenal extensions. Functionality of alginate encapsulated spheroids in vitro. Electron-microscopical analysis of extensions exhibited characteristic of all three adrenal zones: zona Glomerulosa (zG) (A), zona Fasciculata (zF) (B) and zona Reticularis (zR) (C), such as numerous cytoplasmic lipid droplets (L), smooth endoplasmic reticulum (ser), microvilli (mv) and mitochondria (mit). The presence of elongated and oval-shaped cristae-like mitochondria is typical for the zG (D), whereas round mitochondria with typical vesicular internal membrane (E) occurred in the zF cells. Increased number of lysosomes (ly) and enlarged tubovesicular mitochondria representing zR cell (F). A: scale bar 1 μ m, B: scale bar, 5 μ m; C, D, F— scale bar 500 nm, E: scale bar 200 nm. (G) Secretion of cortisol and (H) aldosterone with and w/o ACTH-stimulation. (I) Production of aldosterone with and without angiotensin II (Ang.II) stimulation. (J). Comparative secretion of steroids representing three adrenal zones by cell suspension and spheroids ($n \geq 3$). Statistical significance indicates the disparity between the basal and stimulated levels of steroid hormones. Data are presented as mean \pm SEM. * $p < .05$, ** $p < .01$, *** $p < .001$.

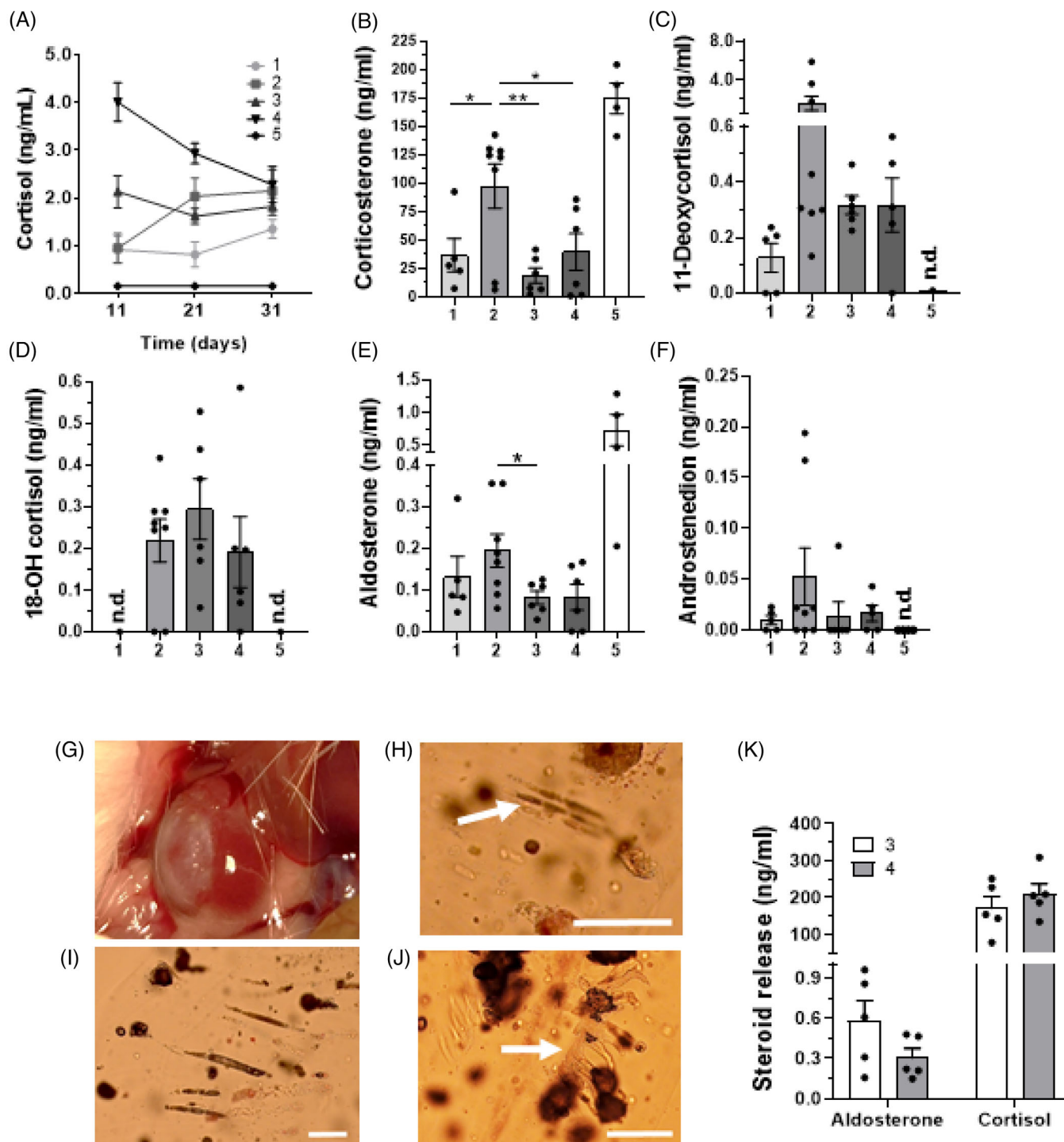


FIGURE 5 Porcine adrenal cells and spheroids transplanted into adrenalectomized SCID mice produce glucocorticoids, mineralocorticoids and androgens. (A) Dynamics of cortisol in mouse plasma after transplantation of (1) cell suspension, (2) naked spheroids, (3) alginate-encapsulated spheroids, (4) spheroids encapsulated in alginate and precultivated for 3 weeks before transplantation ($n \geq 5$); and control mice (5) ($n = 4$). (B–F) Steroid hormones in mouse plasma of all experimental groups, detected by LC-MS/MS analysis at the end point of the experiment (day 31): corticosterone (B), 11-Deoxycortisol (C), 18-Hydroxycortisol (D), Aldosterone (E) and Androstenedione (F) ($n \geq 5$). (G) Transplanted slab in the subcapsular space of a kidney. (H) Adrenal extensions, grown in the slabs after transplantation into mice for 31 days. White arrow indicates adrenal extensions. Scale bar, 100 μm . (I) Group 4—extensions, detached from the source spheroids during transplantation period. Scale bar, 200 μm . (J) Newly formed adrenal tissue in the transplanted alginate slabs in group 4. White arrows indicate newly formed extensions. (K) ACTH-stimulated aldosterone and cortisol production of explanted freshly encapsulated spheroids (group 3) and precultivated before transplantation (group 4) ($n \geq 5$). All data presented as mean \pm SEM. * $p < .05$, ** $p < .01$, *** $p < .001$.

not display increases. Notably, the concentration of cortisol in group 4 showed a progressive decrease.

Significant variations in blood cortisol levels were observed among animals from different experimental groups at day 11 following transplantation. Specifically, group 3 exhibited a significantly higher blood cortisol level compared to groups 1 and 2 ($p < .01$ between group 3 and group 1, and $p < .05$ between group 3 and group 2, respectively). Furthermore, within the experimental groups, group 4 displayed the highest blood cortisol level ($p < .001$ between group 4 and groups 1 and 2, $p < .01$ between group 4 and group 3). At day 21 following transplantation, the blood cortisol levels of animals in both groups transplanted with naked spheroids (group 3) and the group transplanted with precultivated alginate-embedded spheroids (group 4) were found to significantly surpass those of animals in the group transplanted with naked cells (group 1) ($p < .01$ between group 3 and group 1, $p < .001$ between group 4 and group 1). Additionally, animals from group 4 exhibited significantly higher cortisol concentrations compared to those in group 3 ($p < .001$). It is intriguing to note that despite the differences in blood cortisol concentrations observed on days 11 and 21, all four experimental groups displayed similar cortisol levels at the end of the experiment on day 31 ($p > .05$ between all groups). Cortisol in group 5 (control mice) was below the threshold value, as expected. At the same time, all experimental animals showed an equal body weight and behavior (Figure S5C). However, there were noticeable differences in body weight changes between the control group and all transplant groups (Figure S5C). After transplantation, the animals experienced a weight loss, followed by recovery to the initial weight.

The concentrations of glucocorticoids (corticosterone (Figure 5B), 11-deoxycortisol (Figure 5C), and 18-hydroxycortisol (Figure 5D), mineralocorticoids (aldosterone, Figure 5E), and adrenal androgens (androstenedione (Figure 5F) and DHEA (Table S1) in mouse plasma markedly varied among the groups.

Corticosterone secretion was found in all mice (Figure 5B). Experimental animals secreted significantly less corticosterone than the controls (group 5) (174.71 ± 13.54 ng/mL). Animals in group 2 demonstrated significantly higher corticosterone levels compared to other experimental groups.

11-deoxycortisol, one of the precursors of cortisol, was detected in three out of five mice in group 1 (67%), and in all animals in group 2 (8/8, 100%) as well as group 3 (6/6, 100%) (Figure 5C) and in four out of six animals (67%) in group 4. Although 11-deoxycortisol levels were markedly higher in the animals transplanted with naked spheroids, they did not reach statistical significance due to the high variability in the latter group ($p > .1$). 11-deoxycortisol was not detected in the plasma of the control mice (group 5).

18-hydroxycortisol, a cortisol metabolite, was detectable in animals in groups 2, 3, and 4 (Figure 5D). We could not detect 18-hydroxycortisol in mice in group 1 (cell suspension) and control animals (group 5).

Aldosterone secretion was detected in all animals with experimental animals demonstrating significantly lower values than control animals (group 5) (Figure 5E). The plasma aldosterone concentration was comparable between all groups (group 1: 0.13 ± 0.05 ng/mL; group

4: 0.12 ± 0.03 ng/mL; slight elevation in the group 2 (0.19 ± 0.04 ng/mL and a slight reduction in group 3 (0.08 ± 0.02 ng/mL).

Detectable levels of porcine cell-derived adrenal androgens were observed in the experimental animals. Androstenedione was detected in three out of five mice in group 1 (67%), and in five animals in group 2 (5/8, 62.5%), in one mouse in group 3 (1/6, 16.7%), and in three out of six animals (50%) in group 4 (Figure 5F). As expected, androstenedione was not detected in the plasma of control animals. DHEA, the signature porcine adrenal androgen, was detected only in six out of eight mice in group 2 (Table S1).

After explantation, all alginate-encapsulated samples were analyzed microscopically or evaluated for their functional activity (Figure 5G). Slabs of group 3 (alginate slabs with freshly encapsulated spheroids), revealed the formation of column-shaped extensions (Figure 5H), similar to those formed during *in vitro* cultivation. Slabs of group 4 (alginate slabs with spheroids and extensions) showed preserved extensions but detached from the source spheroids (Figure 5I). Moreover, the growth of newly formed extensions was observed (Figure 5G).

The functional activity of the explanted freshly encapsulated spheroids (group 3) and slabs pre-cultivated for three weeks (group 4) was assessed upon 3 h stimulation with ACTH (Figure 5K). We found that regardless of the age of transplanted spheroids, they preserved their functionality during the entire transplantation period. The mean aldosterone concentration of the slabs containing freshly embedded spheroids (group 3) was 0.578 ± 0.154 ng/mL, and for group 4, it was 0.303 ± 0.069 ng/mL, $p > .05$. The average cortisol secretion in group 3 was 171 ± 31 ng/mL, as compared to 209 ± 28 ng/mL in group 4, $p > .05$.

4 | DISCUSSION

In this study, we generated porcine-derived spheroids able to produce glucocorticoids, mineralocorticoids, and adrenal androgens.

Spheroid cultivation is a promising direction in regenerative medicine. The functionality of spheroids depends on the quality of the initial monolayer tissue culture, which changes during the cultivation period. Therefore, in the first step, we defined the optimal time point for the establishment of adrenal spheroids, based on the properties of the primary culture. Primary cultures of adrenal cells consist mostly of mature cells, which produce steroid hormones in response to specific endocrine factors. ACTH-responsiveness of the primary culture is an important parameter, which should be considered when establishing adrenal spheroids. Directly connected to ACTH-sensitivity is the gene expression of the steroidogenic hydroxylases *CYP17A1* and *CYP21*. Our previous work with bovine adrenocortical cells demonstrated a direct connection between the expression of *CYP17A1* in the primary cell culture and the functionality of a 3D bioartificial adrenal cortex model.²⁴

Current models of adrenal cell homeostasis in mice describe various populations of adrenocortical stem and progenitor cells, located in the capsule or the subcapsular region of the adrenal cortex.^{26,27} In mice, cells expressing *Gli1*, *Dax1*, *Wnt4*, *Ctnnb1*, and *Shh* have been shown to participate in the plasticity of the adrenal gland and the formation

of its main structural zones.²⁸ The presence of stem and progenitor cells and their further differentiation into mature steroid-producing cells under the influence of ACTH is a central regeneration mechanism that ensures the formation of a full-fledged adrenal cortex.²⁶ In the present study, during the first 4 days of cultivation, we observed the upregulation of progenitor markers. Taking into consideration the gene expression of steroidogenic hydroxylase *CYP21* and *CYP17A1*, as well as the ACTH-sensitivity of the tissue culture, the time point when the cells are the most suitable for spheroid formation is day 4 after starting the cultivation.

Although conventional 2D cell models have been widely used in the adrenal field to study different aspects of cell biology, cell-cell interactions, and homeostasis, these models failed to restore a complex tissue-specific microenvironment, which significantly reduced their applicability.²⁹ Moreover, monolayer tissue cultures, due to the absence of the tissue-specific architecture, mechanical, and chemical cues, deviated from their parental genomic profile and as a result, have been demonstrated to lose sensitivity toward hormones, growth and differentiation factors.^{29,30} In contrast, upon 3D culture, spheroids partially restored the tissue-specific organization, preserved genome stability, and therefore, genetically were more representative of the organ of origin.^{29–31} Therefore, restoration of fully functioning adrenal tissue is possible on the base of 3D spheroids with high functionality.

For successful long-term functionality of porcine adrenal spheroids, it is crucial that they contain adrenocortical stem and progenitor cells, as these cells can differentiate into fully mature steroid-producing cells. Our research findings indicate the existence of SF-1 positive cells within the spheroids, which mark steroid producing cells. However, a significant proportion of the spheroids lacked SF-1 expression, suggesting the presence of either medullary cells, dedifferentiated adrenocortical cells or SF-1 negative progenitor cells. Our previous data revealed the presence of a substantial number of DAX1 and SHH positive progenitor cells, along with Nestin positive cells.²³ These cells could contribute to the population of SF-1 negative cells. It is plausible that Nestin positive cells may originate from either the medulla or the adrenal cortex.²⁷

Extension formation by spheroids was observed upon their encapsulation in an alginate matrix and induced by ACTH. Interestingly, column-shaped structures are also present in the zF, the ACTH-responsive tissue in the adult adrenal gland.³² Extension formation was not limited to porcine spheroids. Spheroids established from mouse and bovine adrenal cells form similar extensions (data not shown). These structures could only be achieved upon embedding of spheroids in alginate matrix in the form of a slab. Spheroids encapsulated in alginate microcapsules did not form extensions. In our experimental setting, alginate mimics extracellular matrix, providing physical support and a protective environment, necessary for cell growth and differentiation.

In our *in vivo* experiments, we tested the potential advantage of transplanted spheroids over suspension cells to replace all major steroids in the adrenalectomized animals. For these experiments, the immune-deficient SCID mouse model was chosen in order to avoid the impact of the mouse immune system on the xenogeneic mate-

rial. Two groups of animals were transplanted with porcine adrenal spheroids embedded in alginate. In these experiments, the use of alginate had a dual purpose; first, alginate served as an extracellular matrix, where spheroid cells could proliferate and differentiate into adrenal tissue; secondly, alginate acted as an immuno-isolating scaffold providing long-term protection of xenogeneic cells from the recipient immune system, which would be necessary for future trials on immune competent animals. Previous data from our group showed that alginate can protect xenogeneic cells in immunocompetent rodents and reverse the adrenal insufficiency phenotype.¹⁰

During the initial 7 days following adrenalectomy and transplantation, a gradual weight loss was observed in the animals. Subsequently, the animals were only able to regain their initial weight and did not experience further weight gain. These findings align with previous studies that have demonstrated a substantial influence of adrenalectomy on body weight gain in animals.³³

Mice use corticosterone as a main glucocorticoid.¹² In all experimental groups, we could detect cortisol. In contrast and as expected, in the control group (group 5), cortisol was below the threshold value. This observation proves the secretion of steroid hormones by the graft.

While no significant differences were observed between the encapsulated cell suspension and spheroids *in vitro*, our *in vivo* data revealed the superiority of naked spheroids over cell suspension. Specifically, the spheroid group exhibited higher levels of all steroid hormones assessed.

The comparison of cortisol concentrations at different time points after transplantation demonstrated the changes in the grafts' functional status. A gradual increase in cortisol secretion observed in the mice transplanted with naked cells and spheroids could be due to the growth of the transplanted adrenal tissue *in vivo*, previously described by other researchers.³⁴ There, the initial cell aggregation within the host and formation of a vascular system, supporting subsequent survival, growth and function of the transplant tissue was observed.

Additional factors, including variations in cell number, cell maturity at the time of transplantation, and cellular senescence, can influence the functionality of the grafts. Notably, the cell number may differ among the experimental groups. Unlike cell suspension, the naked and freshly alginate-embedded spheroids were transplanted after a 24-h period during which they underwent proliferation. In the case of group 4, the cells proliferated, differentiated, and formed adrenal extensions over a 3-week precultivation period. Furthermore, our *in vitro* data exhibited a significant increase in cortisol production in the slabs after 3 weeks of cultivation compared to freshly prepared ones. Cell senescence could potentially contribute to the decrease in blood cortisol concentration observed in group 4.

Despite observing a significant increase in cortisol production during the initial 4 weeks following the encapsulation of spheroids in alginate *in vitro*, we did not observe a corresponding increase *in vivo*. The cortisol levels of freshly alginate-embedded spheroids remained stable throughout the entire observation period. In our study, we made an interesting observation regarding the formation of extensions, which were noticeably fewer *in vivo* compared to *in vitro* conditions.

Additionally, we identified alginate as a potential barrier between the host's blood vessels and the transplanted adrenal spheroids, which could impede the diffusion of oxygen and nutrients. Our hypothesis suggests that the subcapsular space of the kidney can effectively supply freshly encapsulated spheroids with sufficient oxygen and nutrients. However, as spheroids develop extensions, their increased demand for oxygen and nutrients surpasses the capacity that the subcapsular space can offer. This phenomenon can potentially explain the observed decline in cortisol production in group 4.

The experimental mice exhibited a notable level of corticosterone. The presence of corticosterone could be explained by the adrenal remnant, regeneration of the adrenal tissue,³⁵ or by production by the transplanted cells. Interestingly, the animals, which received naked spheroids, demonstrated the highest corticosterone concentrations as well as the cortisol precursor 11-deoxycortisol produced by transplanted cells. This could be due to the inhibitory effect of alginate on cell proliferation and/or the reduced diffusion of steroid hormones and metabolites,³⁶ which may explain the lower concentrations of corticosterone, aldosterone, and 11-deoxycortisol observed in alginate-encapsulated spheroids compared to naked spheroids.

In all forms of transplantation, the observed aldosterone concentration reached only 15%–30% of the normal levels (Figure 5E). However, these levels appeared to be adequate in replacing the mineralocorticoid function, as evidenced by the animals regaining weight and not exhibiting signs of dehydration (Figure 55C).

The question of whether transplanted porcine spheroids could restore electrolyte balance and circadian rhythm remains unanswered. Insufficient blood samples were obtained from the mice, preventing comprehensive blood-related tests such as LC-MS/MS analysis, electrolyte level measurements, and circadian rhythm analysis.

An equally significant observation is that only adrenal spheroids embedded in alginate were capable of forming extensions, both in vivo and in vitro. It is noteworthy that alginate-encapsulated suspension culture did not exhibit extension formation, which was consistent with our earlier experiments conducted in both in vitro and in vivo settings.^{10,13}

This in vivo experiment demonstrated the advantages of spheroid transplantation over the suspension culture. However, for a potential clinical application, adrenal spheroids should be transplanted in alginate or another biomaterial, or a device with immune protective properties. Moreover, the pre-cultivation of alginate-encapsulated adrenal spheroids before transplantation makes it possible to perform pre-transplantation quality-control tests and to choose potential grafts with high steroid production.

5 | CONCLUSION

This work focused on the formation of an in vitro porcine adrenal model based on alginate-embedded adrenal spheroids and its efficacy in reversing the adrenal insufficiency phenotype in SCID mice after bilateral adrenalectomy. These results may pave the way for future

applications of this improved long-term functional adrenal model as a cell source for an immuno-isolating device for transplantation into immune-competent recipients, as well as for studying adrenal trans-differentiation in vitro and for drug testing.

AUTHOR CONTRIBUTIONS

Maria Malyukov and Evgeny Gelfgat conducted experiments, acquired and analyzed data, Evgeny Gelfgat performed statistical analysis, Stefan R. Bornstein and Barbara Ludwig designed research studies, Barbara Ludwig provided analytic tools, Gerard Ruiz-Babot and Susann Lehmann performed immunofluorescence staining, Maria Malyukov, Evgeny Gelfgat, and Janine Schmid wrote the manuscript, Charlotte Steenblock and Gerard Ruiz-Babot performed imaging and shared ideas, Charlotte Steenblock, Gerard Ruiz-Babot, Felix Beuschlein, Constanze Hantel, Peter P. Nawroth, and Nicole Reisch revised the manuscript

ACKNOWLEDGMENTS

This study was supported by the Deutsche Forschungsgemeinschaft (DFG, German Research Foundation) project no. 314061271, TRR 205: "The Adrenal: Central Relay in Health and Disease", SFB-TRR 127 and KFO 252, the German Academic Exchange Service (DAAD), and the TransCampus initiative between TU Dresden and King's College London. We are thankful to Thomas Kurth, TUD, Center for Molecular and Cellular Bioengineering (CMCB), Technology Platform, EM and Histology Facility for performing electron microscopy, and for providing a facility for microscopy, to Mirko Peitzsch and Denise Kaden for performing the LC-MS/MS analysis and to Linda Friedrich for slide preparation for immunohistochemical analysis.

Open access funding enabled and organized by Projekt DEAL.

CONFLICT OF INTEREST STATEMENT

All authors have no conflict of interest relevant to this manuscript.

ORCID

Maria Malyukov  <https://orcid.org/0009-0008-6966-0521>

Charlotte Steenblock  <https://orcid.org/0000-0002-9635-4860>

REFERENCES

- Chabre O, Goichot B, Zenaty D, Bertherat J. Group 1. Epidemiology of primary and secondary adrenal insufficiency: prevalence and incidence, acute adrenal insufficiency, long-term morbidity and mortality. *Ann Endocrinol (Paris)*. 2017;78(6):490-494. <https://doi.org/10.1016/j.ando.2017.10.010>
- Ueland GA, Husebye ES. Metabolic complications in adrenal insufficiency. *Front Horm Res*. 2018;49:104-113. <https://doi.org/10.1159/000486004>
- Quinkler M, Oelkers W, Remde H, Allolio B. Mineralocorticoid substitution and monitoring in primary adrenal insufficiency. *Best Pract Res Clin Endocrinol Metab*. 2015;29(1):17-24. <https://doi.org/10.1016/j.beem.2014.08.008>
- Rushworth RL, Chrisp GL, Bownes S, Torpy DJ, Falhammar H. Adrenal crises in adolescents and young adults. *Endocrine*. 2022;77(1):1-10. <https://doi.org/10.1007/s12020-022-03070-3>
- Shibuya K, Watanabe M, Goto R, Zaitzu M, Ganchiku Y, Taketomi A. The efficacy of the hepatocyte spheroids for hepatocyte

- transplantation. *Cell Transplant*. 2021;30:9636897211000014. <https://doi.org/10.1177/09636897211000014>
6. Kouroupis D, Willman MA, Best TM, Kaplan LD, Correa D. Infrapatellar fat pad-derived mesenchymal stem cell-based spheroids enhance their therapeutic efficacy to reverse synovitis and fat pad fibrosis. *Stem Cell Res Ther*. 2021;12(1):44. <https://doi.org/10.1186/s13287-020-02107-6>
 7. Akolpoglu MB, Inceoglu Y, Bozuyuk U, et al. Recent advances in the design of implantable insulin secreting heterocellular islet organoids. *Biomaterials*. 2021;269:120627. <https://doi.org/10.1016/j.biomaterials.2020.120627>
 8. Thomas M, Yang L, Hornsby PJ. Formation of functional tissue from transplanted adrenocortical cells expressing telomerase reverse transcriptase. *Nat Biotechnol*. 2000;18(1):39-42. <https://doi.org/10.1038/71894>
 9. Thomas M, Hornsby PJ. Transplantation of primary bovine adrenocortical cells into *scid* mice. *Mol Cell Endocrinol*. 1999;153(1-2):125-36. [https://doi.org/10.1016/s0303-7207\(99\)00070-2](https://doi.org/10.1016/s0303-7207(99)00070-2)
 10. Balyura M, Gelfgat E, Ehrhart-Bornstein M, et al. Transplantation of bovine adrenocortical cells encapsulated in alginate. *Proc Natl Acad Sci USA*. 2015;112(8):2527-32. <https://doi.org/10.1073/pnas.1500242112>
 11. Tanaka T, Aoyagi C, Mukai K, Nishimoto K, Kodama S, Yanase T. Extension of survival in bilaterally adrenalectomized mice by implantation of SF-1/Ad4BP-induced steroidogenic cells. *Endocrinology*. 2020;161(3):bqaa007. <https://doi.org/10.1210/endo/bqaa007>
 12. Gallo-Payet N, Battista MC. Steroidogenesis-adrenal cell signal transduction. *Compr Physiol*. 2014;4(3):889-964. <https://doi.org/10.1002/cphy.c130050>
 13. Balyura M, Gelfgat E, Steenblock C, et al. Expression of progenitor markers is associated with the functionality of a bioartificial adrenal cortex. *PLoS One*. 2018;13(3):e0194643. <https://doi.org/10.1371/journal.pone.0194643>
 14. Robic A, Faraut T, Prunier A. Pathways and genes involved in steroid hormone metabolism in male pigs: a review and update. *J Steroid Biochem Mol Biol*. 2014;140:44-55. <https://doi.org/10.1016/j.jsbmb.2013.11.001>
 15. Lenders JWM, Williams TA, Reincke M, Gomez-Sanchez CE. DIAGNOSIS OF ENDOCRINE DISEASE: 18-Oxocortisol and 18-hydroxycortisol: is there clinical utility of these steroids? *Eur J Endocrinol*. 2018;178(1):R1-R9. <https://doi.org/10.1530/EJE-17-0563>
 16. Yang L, Guell M, Niu D, et al. Genome-wide inactivation of porcine endogenous retroviruses (PERVs). *Science*. 2015;350(6264):1101-4. <https://doi.org/10.1126/science.aad1191>
 17. Fishman JA. Prevention of infection in xenotransplantation: designated pathogen-free swine in the safety equation. *Xenotransplantation*. 2020;27(3):e12595. <https://doi.org/10.1111/xen.12595>
 18. Peitzsch M, Dekkers T, Haase M, et al. An LC-MS/MS method for steroid profiling during adrenal venous sampling for investigation of primary aldosteronism. *J Steroid Biochem Mol Biol*. 2015;145:75-84. <https://doi.org/10.1016/j.jsbmb.2014.10.006>
 19. Kurth T, Berger J, Wilsch-Brauninger M, et al. Electron microscopy of the amphibian model systems *Xenopus laevis* and *Ambystoma mexicanum*. *Methods Cell Biol*. 2010;96:395-423. [https://doi.org/10.1016/S0091-679X\(10\)96017-2](https://doi.org/10.1016/S0091-679X(10)96017-2)
 20. Juznic L, Peuker K, Strigli A, et al. SETDB1 is required for intestinal epithelial differentiation and the prevention of intestinal inflammation. *Gut*. 2021;70(3):485-498. <https://doi.org/10.1136/gutjnl-2020-321339>
 21. Venable JH, Coggeshall R. A simplified lead citrate stain for use in electron microscopy. *J Cell Biol*. 1965;25:407-8. <https://doi.org/10.1083/jcb.25.2.407>
 22. Shi DL, Savona C, Chambaz EM, Feige JJ. Stimulation of fibronectin production by TGF-beta 1 is independent of effects on cell proliferation: the example of bovine adrenocortical cells. *J Cell Physiol*. 1990;145(1):60-8. <https://doi.org/10.1002/jcp.1041450110>
 23. Bornstein S, Shapiro I, Malyukov M, et al. Innovative multidimensional models in a high-throughput-format for different cell types of endocrine origin. *Cell Death Dis*. 2022;13(7):648. <https://doi.org/10.1038/s41419-022-05096-x>
 24. Balyura M, Gelfgat E, Steenblock C, et al. Expression of progenitor markers is associated with the functionality of a bioartificial adrenal cortex. *PLoS One*. 2018;13(3):e0194643. <https://doi.org/10.1371/journal.pone.0194643>
 25. Thomas M, Northrup SR, Hornsby PJ. Adrenocortical tissue formed by transplantation of normal clones of bovine adrenocortical cells in *scid* mice replaces the essential functions of the animals' adrenal glands. *Nat Med*. 1997;3(9):978-83. <https://doi.org/10.1038/nm0997-978>
 26. Finco I, Mohan DR, Hammer GD, Lerario AM. Regulation of stem and progenitor cells in the adrenal cortex. *Curr Opin Endocr Metab Res*. 2019;8:66-71. <https://doi.org/10.1016/j.coemr.2019.07.009>
 27. Steenblock C, Rubin de Celis MF, Delgadillo Silva LF, et al. Isolation and characterization of adrenocortical progenitors involved in the adaptation to stress. *Proc Natl Acad Sci USA*. 2018;115(51):12997-13002. <https://doi.org/10.1073/pnas.1814072115>
 28. Lyraki R, Schedl A. Adrenal cortex renewal in health and disease. *Nat Rev Endocrinol*. 2021;17(7):421-434. <https://doi.org/10.1038/s41574-021-00491-4>
 29. Cui X, Hartanto Y, Zhang H. Advances in multicellular spheroids formation. *JR Soc Interface*. 2017;14(127). <https://doi.org/10.1098/rsif.2016.0877>
 30. Lin RZ, Chang HY. Recent advances in three-dimensional multicellular spheroid culture for biomedical research. *Biotechnol J*. 2008;3(9-10):1172-84. <https://doi.org/10.1002/biot.200700228>
 31. Fennema E, Rivron N, Rouwkema J, van Blitterswijk C, de Boer J. Spheroid culture as a tool for creating 3D complex tissues. *Trends Biotechnol*. 2013;31(2):108-15. <https://doi.org/10.1016/j.tibtech.2012.12.003>
 32. Vinson GP. Functional zonation of the adult mammalian adrenal cortex. *Front Neurosci*. 2016;10:238. <https://doi.org/10.3389/fnins.2016.00238>
 33. Rothwell NJ, Stock MJ, York DA. Effects of adrenalectomy on energy-balance, diet-induced thermogenesis and brown adipose-tissue in adult cafeteria-fed rats. *Comp Biochem Phys A*. 1984;78(3):565-569. [https://doi.org/10.1016/0300-9629\(84\)90597-8](https://doi.org/10.1016/0300-9629(84)90597-8)
 34. Thomas M, Hawks CL, Hornsby PJ. Adrenocortical cell transplantation in *scid* mice: the role of the host animals' adrenal glands. *J Steroid Biochem*. 2003;85(2-5):285-290. [https://doi.org/10.1016/S0960-0760\(03\)00212-7](https://doi.org/10.1016/S0960-0760(03)00212-7)
 35. Gotlieb N, Albaz E, Shaashua L, et al. Regeneration of functional adrenal tissue following bilateral adrenalectomy. *Endocrinology*. 2018;159(1):248-259. <https://doi.org/10.1210/en.2017-00505>
 36. Puguán JMC, Yu XH, Kim H. Diffusion characteristics of different molecular weight solutes in Ca-alginate gel beads. *Colloid Surface A*. 2015;469:158-165. <https://doi.org/10.1016/j.colsurfa.2015.01.027>

SUPPORTING INFORMATION

Additional supporting information can be found online in the Supporting Information section at the end of this article.

How to cite this article: Malyukov M, Gelfgat E, Ruiz-Babot G, et al. Transplantation of porcine adrenal spheroids for the treatment of adrenal insufficiency. *Xenotransplantation*. 2023;30:e12819. <https://doi.org/10.1111/xen.12819>